

Answer to the review of Graham Yielding:

Dear Graham Yielding,

We are very grateful for your kind and helpful review and the recommendation for publication. In the following we answer to the individual issues that were pointed out to increase the quality of the manuscript.

Kind regards,

Michael Kettermann

1. *In this regard, I think a very useful addition to the figures would be explicit SGR results for each section where FW and HW parts of the clay are visible. SGR values are mentioned in places in the text but in a rather approximate way.*

→We agree and add a table summarizing known and estimated SGR value for all cross-sections.

Section	Σ Clay thickness [cm]	Throw [cm]	SGR
1.1	~15(left)/25(right)	48(left)/54(right)	0.3(left)/0.46(right)/0.2(total)
1.2	17	54	0.3
2.1	19	57	0.3
2.2	-	-	-
3.1	-	-	-
3.2	30*	70	0.4
4.1	6	120*	0.05
4.2	20	90	0.2

Table 1: Summary of SGR values in the presented cross-sections. In section 1.1 two fault strands are visible (cf. Fig. 8a), source clay thickness and throw values are given separately and SGR values provided for each fault strand and for the total throw. Estimated values marked with *.

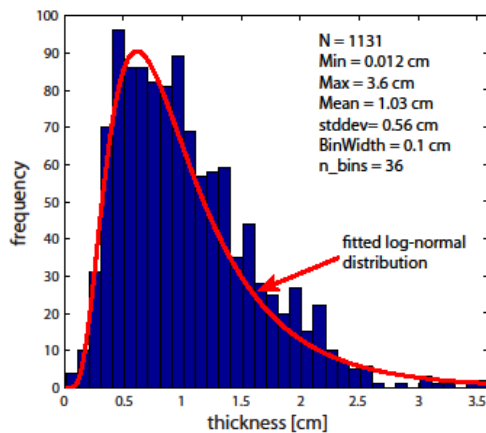
2. *"On page 5, line 16, the comment should be more carefully worded to avoid misinterpretation - I suggest "If we are looking for faults with $SGR < 0.2$, single source clays have to be $< 20\text{cm}$ thick if the fault throw = 1.0m ."*

→Agreed and changed accordingly.

3. *The discussion of Figure 11 (clay smear thickness histogram) should include a consideration of sampling artifacts at the small-thickness end of the distribution. This is analogous to the concerns about fault-population sampling (e.g. Pickering et al 1995) where truncation at small sizes distorts the statistical fit. I would also suggest plotting the fitted log-normal distribution onto the histogram.*

→ This is a good point. We modified the histogram to a more useful bin-size of 1 mm and added the fitted log-normal distribution. We added the following text:

“One has to consider, though, that a sampling bias at the lower end of the range might affect the distribution (e.g. Pickering et al., 1995). Thinner clay smear or holes may appear between sampling points and are then not resolved. However, visual inspection showed no holes in this part of the smear.”



4. In general I feel that it is good to have the discussion/modelling section here in this same paper as the outcrop observations, in contrast to Anonymous Referee #1.

→ We think so as well and keep the manuscript as one work.

5. However, the Matlab model presented on p.13 (lines 6-18) and Figures 19-21 does not seem particularly insightful, so maybe it could be omitted to shorten the paper a little, or moved to a second Appendix.

→ We agree that this model mainly points out some of the relevant parameters for mixing, which are admittedly quite intuitive and this doesn't justify the length of the paragraph with three figures. However, we see a value in pointing this out to the reader as some kind of invitation to further investigate the processes of grain-scale mixing. The details of the model and the figures are not required in the text though and we moved most of it to Appendix B to shorten the main text distinctly.

The shortened paragraph now reads:

“To explore the effect of clay fragment size and rate of mixing on the evolution of sand-clay gouge, we designed a simple simulation (Matlab, 2015; code in online supplement) where circular clay fragments in a sand matrix are subject to homogeneous simple shear. A detailed description and figures of this model can be found in Appendix B. The results show a logarithmic relation between rate of mixing, distance between particles and the strain required to produce an effective seal by mixing. The initial packing will have an influence on the required strain as well as the distribution of mixing (e.g. stronger mixing at the top of clay fragments), however this will be subject of further research.”

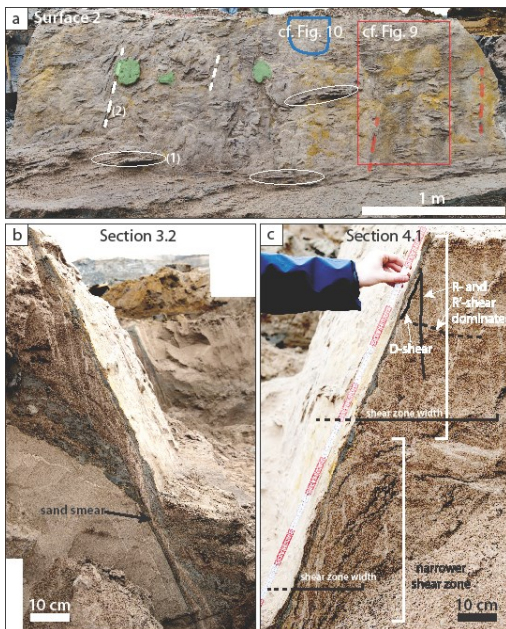
Appendix B now has the three Figures 20, 21 and 22 (now B1, B2 and B3) attached and reads:

*“The general idea of this model is to investigate parameters controlling grain-scale mixing in clay sand sequences. As a basic geometry we chose a number of circular clay fragments with dimensions in the order of mm to cm as observed e.g. in Sample 1.2 (c.f. Fig. 12a) which are embedded in a sand matrix (Fig. B1). This sediment package is then faulted with a certain shear-band width using a simple simulation (Matlab, 2015; code in online supplement). With increasing shear strain a sand-clay mixed seam around the fragments develops and increases in thickness. We ran five series of simulations with initially circular objects representing clay fragments. The rate of mixing is defined as $m = \Delta T / \Delta \gamma$, where ΔT is the change in thickness of the mixed seam per unit shear strain and $\Delta \gamma$ is the change in shear strain. The thickness of the mixing seam at a given shear strain is then $T = \gamma * m$. Simple shear is then applied to the model and shear strain is increased in steps of 0.05. This was done for five distances between clay fragments (0.1, 1, 2, 5 and 10 cm radius) and four rates of mixing (0.001, 0.01, 0.1 and 0.5). Using the ‘intersections’ algorithm (Schwarz, 2010) the code finds the strain at which the ellipses intersect (i.e. clay fragments touch). While a mixing rate of 0.5 is certainly unrealistically high, it serves well for illustrating the procedure (Fig. B2). The results show a logarithmic relation between rate of mixing, distance between particles and the strain required to produce an effective seal by mixing (Fig. B3).”*

Minor technical corrections:

6. p.1, line 12: *sheared not shared* → **changed accordingly**
7. p.2, line 29, insert ‘and’ after ‘faults,’ → **changed accordingly**
8. p.3, line 19, ‘in relays’ not ‘of relays’ → **changed accordingly**
9. p.6, lines 14-16 would be better moved to around line 3, as they are general observations → **Agreed and changed accordingly. Lines 14-16 removed and line 3 ff. now reads: “At first look, both clay smear surfaces contain many sub-horizontal clay ledges with fine horizontal layering locally visible (ellipses labeled (1) in Fig. 5a and Fig. 7a). The clay smear surface is colored by yellowish iron hydroxides. Black striations (dashed lines labeled (2) in Fig. 5a and Fig. 7a) are interpreted to be the result of the fault moving past lignite fragments and they can deviate up to 10° from dip-slip. Vertical sections at both sides of the clay smear are shown in Figure 5b & c and 7b & c.”**
10. p.7, line 21: *R- and R’- shears are absent... there seem to be lots of them on the lower part of Figure 7c. And also, it does NOT seem that the shear zone is wider; refer to interpretation in Fig.13b.*
→ **This is true. We changed the text to: “In the lower part of this section we observe less R’-shears and the D-shear described in the upper part is absent. R-shears and diffuse deformation indicated by sheared lignite seams imply a narrower shear zone compared to the upper part of Figure 7c.”**

Additionally, we modified Figure 7c indicating our interpretation of the shear zone widths and following the suggestions of Reviewer #1 we exemplarily indicated R-, R' and D-shears.



11. p.7, lines 27-28: this sentence refers to Fig.22 and is out of sequence.

→ This sentence is intended to present the data from an additional cross-section (from a different field campaign) to the reader and should be in this paragraph for reasons of completeness. However, to improve the readability and clarity we rephrase the paragraph to: *“Two additional cross-sections are shown in this article from different field campaigns in the same mine and at the same fault and level: (1) Cross-section 5 in Figure 8c (see Fig. 15 for interpretation) shows stair-stepping structures at the footwall side of the clay smear and numerous R-, R'- and D-shears forming two deformed clay smears. (2) We observed a thicker clay smear (~10 cm thickness) with brittle clay fragments entrained into the smear in a cross-section during another field work in 2015 as shown and interpreted in Figure 25a & b.”*

12. p.8, line 8: omit 'with' → changed accordingly

13. p.8, line 10: 'sections 3, 9, 10'....section 9 does NOT show thin smear at the footwall cutoff: perhaps 3, 10 & 11?

→ Yes, you are right, it should be sections 3, 10 and 11. Changed accordingly.

14. p.8, line 19: cast not casted → changed accordingly

15. p.8, line 25-26: I cannot understand this sentence: what is 'footwall cutoff on the hanging-wall side'?

→ We agree that this sentence is confusing. While footwall cutoff should be clear, the hanging-wall side refers to the “upper”-side of the clay smear, i.e. the side of the clay smear

facing the hanging-wall. We rephrase this sentence to clarify: *“At the top of the sample, i.e. the hanging-wall side of the clay smear located at the footwall cutoff, we note the highest sand content that decreases further towards the footwall”*

16. p.10, line 2: *principal not principle* → changed accordingly

17. p.10, line 18: *given that the Kleine Vennekate reference is relatively inaccessible, I suggest that this b/a vs SGR plot be explained more, perhaps in the caption to Fig.17.*

→Yes, this work is unfortunately not yet published in well accessible journal. We extended the description of the method and added a new graphic to aid the understanding. It now reads (Figure numbers don't match the manuscript):

“As stated before there are several empirical methods to predict the sealing potential of clay smears which are based on their actual deformed configuration. These methods are often criticized for overlooking the mechanical and hydraulic behavior of the sealing material. Based on numerical simulations, Kleine Vennekate (2013) proposed a new methodology to evaluate the continuity of the clay smear in a normal fault. This methodology takes into account not only the actual geometry of the deformed clay but also considers the stress state and the shear strength of the low permeable layer.

The evaluation of the stress state and shear strength follows the idea of the MCIP proposed by van der Zee (2003), which infers if the clay deformation occurred under a tension or compression regime for the lowest principal stress (σ_3). The method of Kleine Vennekate (2013) assesses two angles α and β in a principal stress σ_1 and σ_3 diagram shown in Figure 1. Both angles relate the position of the stress state prior deformation to the Mohr Coulomb failure criterion. The angle α links them with the first principal stress axis ($\sigma_3 = 0$) whereas β relates the stress state and the Mohr Coulomb criterion with the estimated stress path during deformation (horizontal line). A ratio $\frac{\beta}{\alpha} < 1$ implies that σ_3 will be negative during the deformation, otherwise σ_3 will be positive. Figure 1 shows an example of two points with different stress states and different $\frac{\beta}{\alpha}$ ratios. The deformed configuration is considered by using the shale gouge ratio. Both criteria, $\frac{\beta}{\alpha}$ and SGR, are then plotted together with a curve that marks the limit between a continuous and discontinuous clay gouge.

This methodology was followed to assess the continuity of the clay gouge in the excavated fault. Figure 2 and 3 show in a principal stress diagram (σ_1, σ_3) the Mohr-Coulomb limit state line and the assumed stress path together with the angles β and α for $c=30\text{kN/m}^2$ $\varphi = 9^\circ$ and $c=90\text{kN/m}^2$ $\varphi = 16^\circ$ respectively. The ratio $\frac{\beta}{\alpha}$ found can vary from a value of 8 up to a value of 28, implying that the value of σ_3 was positive during the deformation.

The continuity of the clay smear is then evaluated in figure 4. Here the limit between continuous and discontinuous clay smear is presented with the continuous line and the calculated upper and lower limit of both SGR and $\frac{\beta}{\alpha}$ are plotted with dashed lines. The shaded area represents all the possible combinations of SGR and $\frac{\beta}{\alpha}$. According to Kleine Vennekate (2013) it can be expected that the clay

smear would be continuous since this area is above the limit curve, the continuous clay smear zone, which is in agreement with the field observations.”

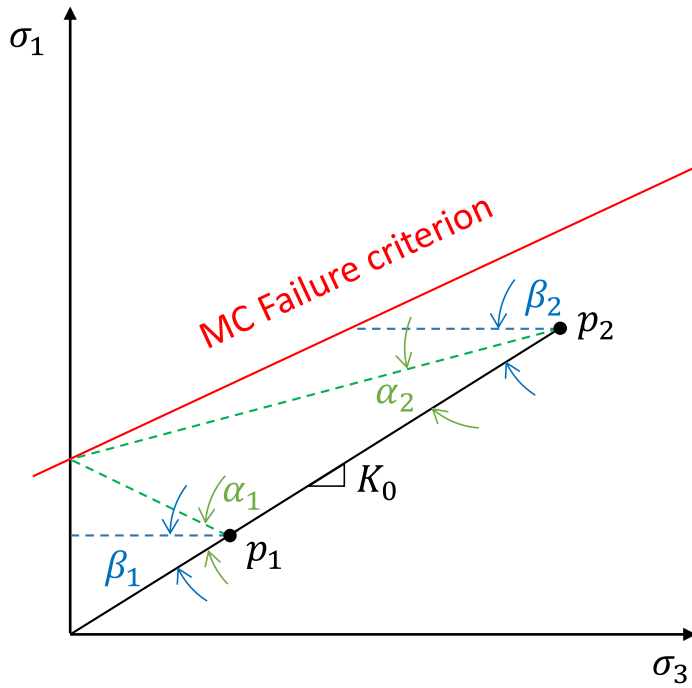


Figure 1: Definition of parameters α and β and estimation of $\frac{\beta}{\alpha}$ ratios for different stress states. Point 1 (p_1) has a ratio $\frac{\beta}{\alpha} < 1$ meaning σ_3 is negative, whereas Point 2 has a ratio of $\frac{\beta}{\alpha} > 1$, meaning positive σ_3 . Red line: Mohr-Coulomb failure criterion, blue dashed lines: stress-path during faulting, green dashed lines: connects beginning of the stress-path during faulting (i.e. p_1 or p_2) with the intersection of the failure criterion and the σ_1 axis.

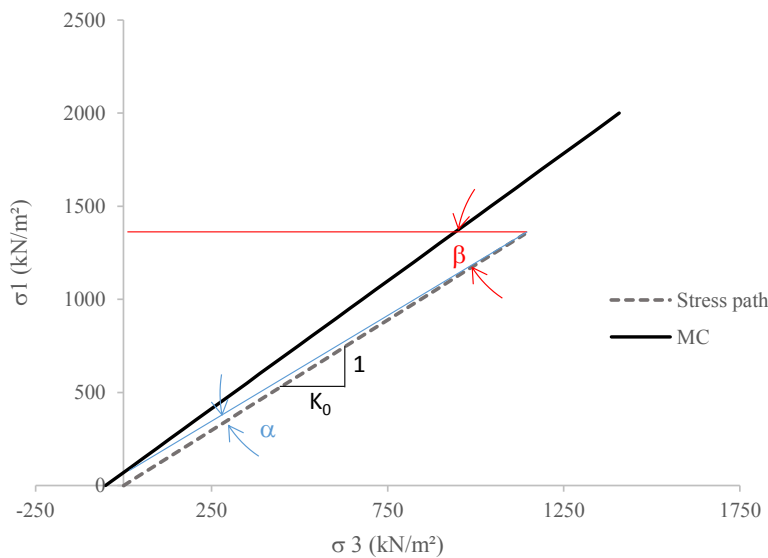


Figure 2: Estimation of β and α for $c=30\text{kN/m}^2$ and $\phi = 9^\circ$. Ratio of $\frac{\beta}{\alpha} > 1$, meaning positive σ_3 .

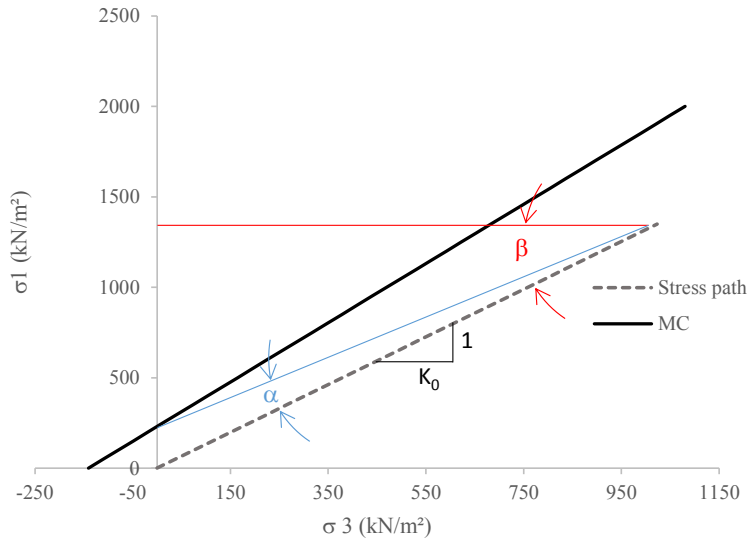


Figure 3: Estimation of β and α for $c=90 \text{ kN/m}^2$ $\varphi = 16$. Ratio of $\frac{\beta}{\alpha} > 1$, meaning positive σ_3 .

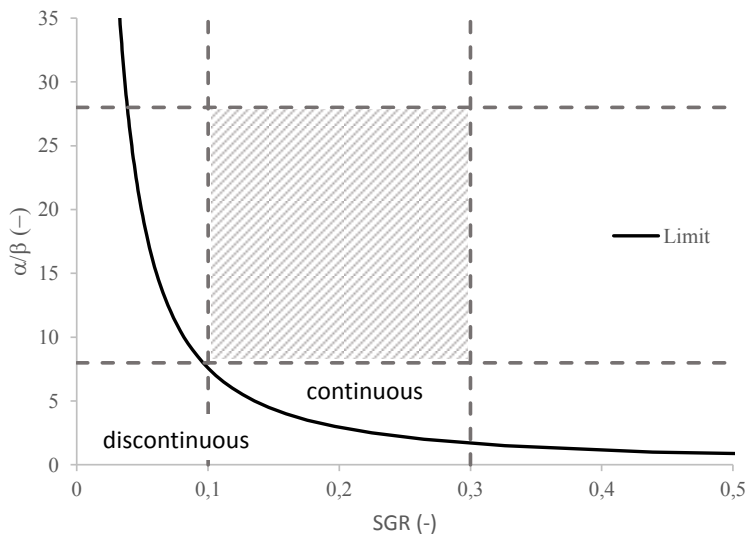


Figure 4: Evaluation of the continuity of the clay smear after Kleine Vennekate (2013). Shaded area represents all possible combinations of SGR and $\frac{\beta}{\alpha}$ for the presented data.

18. p.13, line 4: insert 'implies' after 'smear' → changed accordingly

19. p.15, line 2: than not as → changed accordingly

20. p.15, lines 7-8: meaning unclear, please re-write

→ Yes, something went wrong there. We rephrased to ***“We report observations for faults in this study that are one to two orders of magnitude smaller than those described by Eichhubl et al. (2005), Faerseth (2006) or Aydin and Eyal (2002) but share similar characteristic structures. Thus we hypothesize that detailed observations on small scale faults can be transferred to faults at least one order of magnitude larger.”***

21. Figure 6a, very pretty, but please state in the caption that the colors have been added to improve clarity!

→ The caption now reads: ***“(a) Detail of the SE side of surface 1 showing multiple thin clay veneers composing the bulk clay smear. Colors added manually to distinguish different clay layers.”***

22. Figure 9: make part (e) exactly the same size as the red box in part (d), to improve the reader’s ability to match up features in the two images

→ Agreed and done.

23. Figure 13: in agreement with Referee #1, improve annotation of D-shear

→ Additionally to the legend we added labels for R-, R'- and D-shears to the interpreted image.